ELSEVIER

Biophysical Chemistry 51 (1994) 167-192

Biophysical
Chemistry

Review

A view of thermodynamics of hydration emerging from continuum studies

Alexander A. Rashin [a], Michael A. Bukatin [b]

[a] BioChemComp Inc., 543 Sagamore Ave., Teaneck, NJ 07666, USA
[b] Computer Science Department, Brandeis University, Waltham, MA 02254, USA

Abstract

Main physical–chemical features of hydration found in continuum studies and possible limitations of the method are analyzed. Particular attention is given to: the choice of thermodynamic observables to be compared to the calculations; representations of the solute polarizability; compensation between the loss of hydration enthalpy and gain in Coulomb interactions upon a complex formation; two minima in interaction potentials between polar groups in solution; similarities and dissimilarities between interaction potentials in solution from continuum and molecular theories; continuum calculations of entropies of hydration; and evaluation of a temperature dependence of thermodynamic characteristics of hydration with continuum methods.

Key words: Thermodynamics; Hydration; Continuum studies

1. Introduction

Continuum methods [1,2] came a long way to becoming a respected method in theoretical studies of the solution thermodynamics. Only seven to eight years ago molecular simulation techniques [3–6] solidly dominated the field with integral equation techniques [7] trailing as a distant second. Continuum methods were looked upon with a suspicion at best, with most researchers unable to believe that a simple model could faithfully reproduce energetics of complex molecular systems. However, from 1985 results demonstrating a remarkable success of continuum models in reproducing the energetics of hydration started to accumulate. In 1985 it has been shown [8] that a physically transparent continuum model with only one parameter obtained from fitting to experimental data for alkali-halide salts allows prediction of hydration enthalpies of over 30 spherical ions within a few percent of their experimental values. In 1987 a similar degree of success has been achieved for nonspherical ions [9]. Results, demonstrating similarities of potentials of mean force between oppositely charged spherical ions [10] and hydration energies from continuum models and molecular simulations [1,11] followed. Solute polarizabilities have been incorporated in the continuum formalism [1,12]. More recently it has been shown that continuum models can yield good results in computations of entropies of hydration as well [13–15]. A number of groups joined in a pursuit of quantitative results in hydration thermodynamics via continuum calculations [16–18]. Many different algorithms has been developed for continuum calculation based on

SSDI 0301-4622(94)00060-W

the boundary element technique [1,9,19,20], finite difference technique [21,22], and finite element technique [23] [#1,2]. The number of publications based on the use of continuum models for evaluation of hydration effects for small molecules, proteins and nucleic acids greatly increased and is reflected in an unusually large number of reviews of the approach [1,2,26-31]. As continuum methods became or are becoming a routine tool for thermodynamic studies, it is time, in our opinion, to thoroughly examine possible limits of these methods. The question of limits of accuracy in reproducing experimental results by continuum methods is addressed in another publication [32] in this Issue. Here we concentrate on main features of the physical picture of hydration thermodynamics emerging from continuum studies, and on instances in which the continuum method seems to produce strange results or fail.

The continuum approach already succeeded far beyond any predictions of its critics. We, of course, realize that this approach, based on simple physical ideas, cannot by its design provide the wealth of structural detail available from molecular simulations and theories. This, however, may have its advantages often providing a clear uncluttered physical picture. In our view all approaches, quantum, molecular simulations, or continuum, have their distinct place in the studies of hydration and have their limitations. These should be honestly explored to make further progress possible, or to mark areas in which applications of a particular method are likely to lead to erroneous results at a given stage of its development.

2. Fundamentals of the approach

2.1. Physical model

In our description of the physical model behind continuum approaches we follow refs. [1,2,15,29,30,33,34]. Two groups started to systematically pursue *quantitative* applications and studies of the physics of continuum methods earlier (ours - from 1987 [9], and Honig's - from 1988 [16]) and did it more extensively than other researchers in the field [#3]. Thus, in our analysis of particular choices made in implementations of the physical model we shall concentrate on the use of the boundary element method (BEM) in our group [1,15] and of the finite difference method (FDM) as used by Honig's group [2,29].

Most of the continuum approach is based on a direct or indirect solution of the Poisson equation

$$\nabla[D(\boldsymbol{r})\Delta\varphi(\boldsymbol{r})] + 4\pi\rho(\boldsymbol{r}) = 0, \tag{1}$$

where $D(\boldsymbol{r})$, $\rho(\boldsymbol{r})$ and $\varphi(\boldsymbol{r})$ are the dielectric constant, charge distribution, and potential at point $\boldsymbol{r}$ (here we ignore salt contributions which are relatively small in the thermodynamics of hydration [35]). A direct solution can be obtained in the form of the potential $\varphi(\boldsymbol{r})$ using FDM [2,29] or FEM (finite element method) [23], or with BEM [20]. Indirect solutions are based on the theorem that the total potential in inhomogeneous media can be represented by the sum of potentials of: (a) a charge distribution of the molecule, and (b) of the fictitious 'polarization charges' on dielectric boundaries of the inhomogeneous media. The indirect solution in the form of surface polarization charges can be most naturally obtained with BEM [1,9,19],

$$\sigma(\boldsymbol{r}) = \frac{1}{4\pi}\frac{D_{\text{in}} - D_{\text{out}}}{D_{\text{in}}}E_{\text{out}}(\boldsymbol{r}) \cdot \boldsymbol{n}(\boldsymbol{r}), \tag{2}$$

where $\boldsymbol{n}(\boldsymbol{r})$ is an outside directed normal to the boundary at some point, $\boldsymbol{r}$, and $E_{\text{out}}(\boldsymbol{r})$ is the

---

[#1] We note that modern studies of hydration with continuum reaction fields have been started by Tomasi's group, while this group did not pursue quantitative studies and concentrated on combinations of a crude version of BEM with SCF quantum calculations. For a review and refs. therein see ref. [24].

[#2] The work from Trular's group stands somewhat apart from our subject: while it uses a classical model in conjunction with semiempirical quantum mechanics for evaluation of hydration free energies, it does not directly use classical reaction fields obtained from numeric solutions of Poisson or Poisson-Boltzmann equations but some heavily parametrized empirical substitute of it, making it less physically transparent. See ref. [25].

[#3] In fact, current revival of quantitative continuum studies can be traced back to ref. [8] which, however, did not employ numeric methods characteristic for the present state of the continuum methodology.

electric field at the point $\boldsymbol{r}$ on the surface of the boundary. $\boldsymbol{E}_{\text{out}}$ has contributions from the charge distribution of the solute, $\boldsymbol{E}_{\text{su}}$, and from polarization charges on all boundary elements, $\boldsymbol{E}_{\sigma}$, and from dipoles induced on solute atoms, $\boldsymbol{E}_{\mu}$, and D_{in} and D_{out} are dielectric constants of the medium inside and outside of the dielectric boundary (the formalism for a general case where D_{in} and D_{out} can depend on $\boldsymbol{r}$ is considered in ref. [12], but we do not concentrate on it here). Thus, the indirect method leads to a system of integral equations for unknown surface densities of polarization charges and dipoles, $\boldsymbol{\mu}_j$, induced on atoms

$$\begin{aligned}\sigma(\boldsymbol{r}) = \frac{1}{4\pi}\left(\frac{D_{\text{in}} - D_{\text{out}}}{D_{\text{in}}}\right)\Bigg[&\int_s \frac{\sigma(\boldsymbol{r}')(\boldsymbol{r}-\boldsymbol{r}')\,\mathrm{d}s}{|\boldsymbol{r}-\boldsymbol{r}'|^3} \\ &+ \sum_i \frac{q_i(\boldsymbol{r}-\boldsymbol{r}_i)}{|\boldsymbol{r}-\boldsymbol{r}_i'|^3} \\ &+ \sum_j \left(\frac{3\boldsymbol{\mu}_j\cdot(\boldsymbol{r}-\boldsymbol{r}_j)}{|\boldsymbol{r}-\boldsymbol{r}_j|^5}(\boldsymbol{r}-\boldsymbol{r}_j) \right. \\ &\left. - \frac{\boldsymbol{\mu}_j}{|\boldsymbol{r}-\boldsymbol{r}_j|^3}\right)\Bigg]\cdot\boldsymbol{n}(\boldsymbol{r}), \end{aligned} \tag{3}$$

$$\begin{aligned}\boldsymbol{\mu}_j(\boldsymbol{r}) = \alpha_j\Bigg[&\int_s \frac{\sigma(\boldsymbol{r}')(\boldsymbol{r}_j-\boldsymbol{r}')\,\mathrm{d}s}{|\boldsymbol{r}_j-\boldsymbol{r}'|^3} \\ &+ \sum_i f_q(\boldsymbol{r}_j-\boldsymbol{r}_i)\frac{(\boldsymbol{r}_j-\boldsymbol{r}_i)}{|\boldsymbol{r}_j-\boldsymbol{r}_i'|^3} \\ &+ \sum_{m\neq j} f_\mu(\boldsymbol{r}_j-\boldsymbol{r}_m) \\ &\times\left(\frac{3\boldsymbol{\mu}_m\cdot(\boldsymbol{r}_j-\boldsymbol{r}_m)}{|\boldsymbol{r}_j-\boldsymbol{r}_m|^5}(\boldsymbol{r}_j-\boldsymbol{r}_m) \right. \\ &\left. - \frac{\boldsymbol{\mu}_m}{|\boldsymbol{r}_j-\boldsymbol{r}_m|^3}\right)\Bigg], \end{aligned} \tag{4}$$

where integration is over the surface, s, with differential elements $\mathrm{d}s$; the vacuum charge distribution of the solute is represented by a set of point charges located at some points, $\boldsymbol{r}_i$, not necessarily restricted to the nuclei; induced point dipoles, $\boldsymbol{\mu}_j$, are located on another set of n_μ points, $\boldsymbol{r}_j$, also not necessarily restricted to the nuclei; α_j are point polarizabilities (usually assigned to atoms and/or bonds); and functions $f_q(\boldsymbol{r}_{ij})$ and $f_\mu(\boldsymbol{r}_{jm})$ are discussed below.

A discretization of the dielectric boundary into a set of n_e surface boundary elements and rearrangement of terms leads to a system of $(n_e + 3n_\mu)$ linear algebraic equations for densities of surface polarization charges, σ_i $(1 \leqslant i \leqslant n_e)$, and Cartesian components of induced dipole moments, μ_j^k $(k = x, y, z;\ 1 \leqslant j \leqslant n_\mu)$. The differential Eq. (2) is also discretized and reduced to a system of linear algebraic equations for the values of potentials, φ_i, on the grid nodes. The corresponding systems of equations can be found in refs. [32,36] in this Issue or in more detail in the original papers [1,2,9]. It has been found that for problems dealing with the energetics of hydration it is advantageous to recast even FDM potentials, φ_i, in terms of the surface densities of polarization charges σ_i, [21,36]. Thus, if we ignore effects of the ionic strength, and set all point polarizabilities, α_j (and consequently all induced point dipoles $\boldsymbol{\mu}_m$), to zero, the electrostatic contributions to the free energy of hydration, ΔG_{el}, in both methods can be expressed as

$$\Delta G_{\text{el}} = \tfrac{1}{2}\left(\sum_i q_i \sum_j \sigma_j S_j / |\boldsymbol{r}_i - \boldsymbol{r}_j|\right), \tag{5}$$

where $\boldsymbol{r}_i$ is the position of charge q_i, and $\boldsymbol{r}_j$ is a point on a boundary element with the surface area S_j (these elements can be the same as in the discretization of Eqs. (3) and (4) be their parts or their combinations: we do not discuss these technical details here). If the cavity radii determining the position of the dielectric boundary and the partial charges used by both techniques are the same, their results should also be the same. Any differences under these circumstances are due to numerical errors characteristic for a particular numerical method or its implementation.

It is worth noting here that we have found [1,8,9] from the analysis of electron density maps in ionic crystals that cavity radii for positively charged atoms should be similar to their covalent radii, while for negatively charged atoms cavity radii should be similar to their ionic (or, which is equivalent, van der Waals) radii. It follows from these rules that cavity radii for atoms without significant partial charges (or without an ability to form hydrogen bonds) should be approximately 0.6 Å larger than their van der Waals radii [1,9]. Thus, according to refs. [1,8,9] cavity radii are similar to van der Waals radii only for negatively charged atoms. This asymmetry of cavity radii in respect to the van der Waals radii seems to have a number of important consequences (see below). Many recent publications (e.g., [2,17]) adopt van der Waals radii from some empirical force field as the cavity radii. This may lead to a loss of the above discussed asymmetry and consequently of physically meaningful effects.

2.2. *The choice of thermodynamic observables*

ΔG_{el} is the free energy and not, for example, enthalpy, because both the dielectric constants and cavity radii that determine the position of the dielectric interface depend on temperature (ref. [1] and references therein, [37]). Thus, a temperature derivative of ΔG_{el} at constant cavity radii is the entropy of hydration, ΔS_D, due to the temperature dependence of the dielectric constant, D; a temperature derivative of ΔG_{el} at constant D is the entropy of hydration due to the temperature dependence of the cavity radii, ΔS_r (see footnote 1). $T\Delta S_D$ is ≈ 0.0177 of ΔG_{el} if one assumes that the dielectric constant inside the solute $D_{in} = 1$ and that the temperature dependence of the dielectric constant of water near the solute is well described by its bulk value [1,9]. The latter is not necessarily the case but it is usually assumed to be true in the literature (e.g., see ref. [37]). ΔS_r is of the order of 0.02 of ΔG_{el} for water, and about an order of magnitude smaller for ionic solutes, as estimated from the thermal expansion coefficients of water and ionic crystals correspondingly [1]. While it is again unclear whether the bulk values faithfully reproduce thermal expansion near the solutes in water, these corrections seem to be small compared to ΔG_{el}. At the same time hydration entropies of polar uncharged molecules are of the same order as ΔG_{el} [32], and for ions they constitute about 8% of ΔG_{el} [1], which is a few times larger than ΔS_D. Thus, the question arises of how to compare calculated ΔG_{el} to measurable thermodynamic characteristics of hydration.

A suggestion found in the literature more often is to assume that the measured free energy of hydration, ΔG^0, should be considered as a sum of ΔG_{el} and of other 'non-polar' contributions to the free energy of hydration, ΔG_{np} [31]. The latter term is derived from the data on gas to water transfer of non-polar molecules and is usually assumed to be determined exclusively by their accessible surface areas. It is assumed that this non-polar contribution is the same for polar and non-polar molecules with the same accessible areas [29,31], and can be further divided into the contributions from van der Waals interactions, ΔG_{vdW}, and those from the cavity formation, ΔG_{cav},

$$\Delta G^0 = \Delta G_{el} + \Delta G_{np} = \Delta G_{el} + \Delta G_{vdW} + \Delta G_{cav}. \tag{6}$$

It is doubtful that this decomposition is generally valid. First of all physical processes leading to ΔG_{cav} are rather different for the transfer of non-polar and polar molecules. Water molecules cannot any more form hydrogen bonds in the direction occupied by a non-polar solute. On the other hand, polar solutes (and especially small ions) can replace water–water hydrogen bonds by either equally strong or even stronger water–ion bonds [30]. Thus, there is no a priori reason to assume that the cavity term does not change with a change of the solute charge or that such a change is compensated (either exactly or almost exactly) by a part of ΔG_{el}. This concerns both enthalpic and entropic contributions to ΔG_{cav}.

Similar problems arise in ΔG_{vdW}, which is favourable for gas to water transfer of nonpolar solutes and should be unfavourable at least for transfer of small ions. The latter can be the result of a methodological problem: if total water–ion interaction is a sum of only the electrostatic (Coulomb) and van der Waals terms then the minimum energy at a finite separation can be achieved only at a point where the decrease in the electrostatic energy is compensated by the increase in the repulsion. At the equilibrium separation the repulsion can be quite significant. In fact, 'van der Waals' in empirical force fields stands for a large number of quantum-mechanical terms (exchange, repulsion, polarization, charge transfer and penetration in the second order perturbation theory [30, and references therein]) that are partially compensating.

Thus, if ΔG^0 is chosen as an observable to which the calculated results are compared, one is faced with doubtful transferability of characteristics from nonpolar to polar solutes and has to compensate for it by fiddling with the position of the boundary (cavity radii) and/or with the charge distribution of the solute. Such fiddling may lead to a reasonable agreement between the experimental and the calculated value but may compromise the physical-chemical foundations of the calculation. This may lead to a failure when the same procedure and parameters are applied in a somewhat different structural context. And one would not know what is wrong.

We have chosen a different path which, of course, has its own problems. We attempt to calculate solute charge distributions with a high quality quantum mechanics [32,36] that reproduces experimental vacuum multipole moments (only experimental dipole moments are usually available). Because, as discussed above, the entropic contribution to ΔG_{el} (eq. 5) comprises only a few percent, we correct ΔG_{el} by these few percent to obtain the electrostatic contribution to the enthalpy of hydration, ΔH_{el} [1,9,30]. Note that, as discussed above, for ions only the temperature dependence of the dielectric constant contributes to this correction significantly. For polar uncharged molecules the value of ΔG_{el} is usually below 10 kcal/mol and, thus, a few percent error in its evaluation corresponds to only a few tenths of a kcal/mmol. (Note, of course, that these estimates of the magnitude of corrections are based on the assumptions of the physical model described in the previous section).

It is obvious that a molecule transferred to water from vacuum will have van der Waals interactions with water in addition to the electrostatic interactions. The energy (enthalpy) of the solute-water van der Waals interactions, ΔH_{sw}, can be more easily computed for any solute than ΔG_{np}. Unfortunately, enthalpy change due to the water reorganization in the transfer, ΔH_{re}, appears to be more elusive computationally (e.g. [13]). However, it equally contributes to both ΔG_{np} and to the total enthalpy of hydration, ΔH^{tot}. It is usually assumed that it is positive but small in the transfer of small nonpolar solutes, and is accounted for as the electrostatic energy of the solvent polarization in transfer of small ions [30, and references therein]. The situation may be more complicated in hydration of large solutes where corrections to ΔH_{re}, $\Delta\Delta H_{\mathrm{re}}$, may become significant.

We have recently demonstrated that entropies of hydration, ΔS_{h}, can also be calculated with the help of continuum methods [13-15] and seem to be simple functions of the accessible areas of solutes in gas to water transfer at constant pressure [32] (see also below). Calculated values of ΔS_{h} can be directly compared to the corresponding experimental values, ΔS^0 [32]. Thus, within our approach, the free energy of hydration, ΔG^{tot}, can be expressed as

$$\Delta G^{\mathrm{tot}} = \Delta H_{el} + \Delta H_{\mathrm{vdW}} + \Delta H_{\mathrm{re}} - T\Delta S_{\mathrm{h}} \qquad (7)$$

The free energy of hydration calculated with Eq. (7) can be compared to the corresponding experimental value, ΔG^0. Note that only ΔH_{re} may be difficult to calculate, but it can be assumed negligible for small solutes. At the same time we compute three observables that can be checked against experimental data in contrast to only one observable in approaches currently focused on implementations of Eq. (6) (e.g., see refs. [29,31]). We expect that our approach including more observables (Eq. (7)) may allow a better understanding of discrepancies that may arise in various applications.

2.3. Representations of the solute polarizability

Differences between FDM and BEM formulations start to arise when one attempts to incorporate into the formalism the polarizability of a solute or its parts in the electric field of its other parts or in the reaction field of the solvent. Such attempts also lead to distinct problems characteristic for each technique.

Within the FDM formulation [34] solute polarizability is represented by solute's dielectric constant, $D_{\rm in}$ (usually $D_{\rm in}$ is assumed to be in the range of 2 to 4). Partial charges of a polar uncharged solute will polarize it, and if $D_{\rm in}$ is larger than $D_{\rm out}$ the induced dipole, $\boldsymbol{\mu}_{\rm ind}$, will be directed against the initial dipole, $\boldsymbol{\mu}_{\rm ch}$, due to the partial charges [34]. It is suggested to increase (by scaling) partial charges assigned to atoms so that the sum of new $\mu'_{\rm ch} = \mu^{\rm n}$ (in the notation of ref. [34]) and new $\mu'_{\rm ind}$ equals to the experimental vacuum dipole moment [34]. It can be noted that for asymmetric solutes $\mu_{\rm ind}$ may have different orientation than $\mu_{\rm ch}$, and thus the new 'vacuum' dipole moment $(\boldsymbol{\mu}^{\rm n} + \mu'_{\rm ind})$ may have different orientation than the original dipole, $\boldsymbol{\mu}_{\rm ch}$, from the partial charges in vacuum. Additional problems may arise in calculations of interactions of groups now characterized by partial charges yielding dipoles for these groups equal to $\mu^{\rm n}$ in the medium with the same dielectric constant $D_{\rm in}$. The minimum energy of interaction in vacuum of two identical dipoles characterized by point polarizabilities α is [33]

$$W_{1-2} = \frac{\mu_{\rm ch}^2}{r_{12}^3}\,\frac{-2}{1-2\alpha/r_{12}^3}. \tag{8}$$

If these two dipoles are in cavities of radius a in the dielectric with the dielectric constant $D_{\rm in}$, then at large separation between the cavities they would interact as point dipoles through the dielectric. However, each dipole would increase due to its polarization by the reaction field of the solvent [33]

$$\mu^* = \mu_{\rm ch}\Big/\left[1-\frac{\alpha}{a^3}\,\frac{2(D_{\rm in}-1)}{(2D_{in}+1)}\right] \tag{9}$$

A substitution of the continuum expressions for α [33,34]

$$\alpha = a^3(D_{\rm in}-1)/(D_{\rm in}+2) \tag{10}$$

leads to

$$\mu^* = \mu_{\rm ch}\Big/\left[1-\frac{(D_{\rm in}-1)}{(D_{\rm in}+2)}\,\frac{2(D_{\rm in}-1)}{(2D_{\rm in}+1)}\right]. \tag{11}$$

The interaction energy, $W_{1-2}^{D_{\rm in}}$, of these polarized dipoles in the dielectric is

$$W_{1-2}^{D_{\rm in}} = \frac{-2\mu_{\rm ch}^2}{D_{\rm in}r_{12}^3}\Big/\left[1-\frac{2(D_{\rm in}-1)^2}{(D_{\rm in}+2)(2D_{\rm in}+2)}\right]^2. \tag{12}$$

According to ref. [34] $\mu^{\rm n} = \mu_{\rm ch}(2 + D_{\rm in})/3$. Therefore, the interaction energy of two $\mu^{\rm n}$ dipoles in the dielectric characterized by the same dielectric constant $D_{\rm in}$ is

$$W_{1-2}^{D_{\rm in}} = \frac{-2(\mu^n)^2}{D_{\rm in}r_{12}^3} = \frac{-2\mu_{\rm ch}^2}{D_{\rm in}r_{12}^3}\,\frac{(D_{\rm in}+2)^2}{9}. \tag{13}$$

Thus, the parametrization within two methods providing the same vacuum dipole moment and hydration energy of the individual group leads to a rather different asymptotic behaviour of the energy of interaction of two such groups (Eq. (12) for BEM and Eq. (13) for FDM) (the ratio is ≈ 1.5 for $D_{\rm in} = 2$, and it is 2 for $D_{\rm in} = 4$, with larger absolute values always yielded by Eq. (13)). There may be some way out of this apparent inconsistency, but it was not elaborated in ref. [34] and we are not aware of it (the difference in the reference hydration energy of two infinitely separated groups in two descriptions does not change the asymptotic behaviour). Other problems may arise in a consistent treatment of interactions of multiple polarizable groups in complex molecules, but we do not attempt their analysis here. It is clear, however, that partial charges of a solute obtained from quantum calculations do not polarize this solute (i.e. we do not need to account for such polarization classically). All polarization by the partial charges is already accounted for by the quantum calculation that yielded these partial charges. Problems arise precisely because we try to treat the solute both as a quantum mechanical system (when we obtain its charges) and as a classical continuum dielectric. This dichotomy is difficult to avoid because a classical description *is required* for large systems.

Problems of different sort arise in methodologies ascribing point polarizabilities to atoms or bonds. Our Eqs. (3)–(4) are a particular implementation of such a methodology. Attempts to resolve these problems are reflected in the 'damping' functions $f_q(r_{ij})$ and $f_\mu(r_{jm})$ in Eqs. (3) and (4). These functions reduce ('damp') electric fields respectively of charges and dipoles inducing point dipoles. The 'damping' functions reduce polarizing electric fields at very short separations or allow 'to switch off' interactions between particular points. A necessity of 'damping' for dipole-dipole interactions has been demonstrated by Applequist [38] and implemented by Thole [39]. Recently it has been suggested that different and steeper function should be used for a partial-charge to induced dipole interactions [40]. An example of a 'switch off' can be found in ref. [41] where $f_\mu(r_{jm}) = 0$ for pairs of covalently bonded atoms. In another example both functions were set to zero for all pairs of centers (of partial charges and induced dipoles) within a solute whose partial charges were obtained from quantum-mechanical calculations [1,32]. However, it is not clear whether such 'damping' functions or even the classical description utilizing point polarizabilities truthfully reflects the physical reality.

We have calculated hydration enthalpies and solvent induced dipoles of four dipolar molecules using hybrid quantum-mechanical + reaction-field approach [36]. The calculations [36] yielded good agreement with experimental hydration enthalpies and the solution dipole moment of water in a close agreement with experimental estimates [1]. Calculations of the same observables with our BEM based method utilizing additive point polarizabilities from ref. [42] yielded a similar agreement between the calculated and experimental hydration enthalpies, but the calculated solution dipole moments were systematically larger than the corresponding values from our hybrid quantum calculations (see Table 1). The classically calculated solution dipole moments of water and methanol are ≈ 0.2 D larger than the respective results from our hybrid calculations [36]. The corresponding differences for ammonia and methylamine in Table 1 reach 0.5 D. Even the choice of a smaller (and apparently less proper) polarizability value for the nitrogen reduces the discrepancy for ammonia only to the level found for water and methanol (≈ 0.2 D). Is the scheme of additive polarizabilities inaccurate? May it imply that the dielectric response is not linear as expected in the classical electrostatics? Or may be quantum DFT calculations that we employed [36] are not accurate enough? We look into these equations, but answers are not available yet. The 'damping' functions should also closely correspond to some reality, but this may be even more difficult to pinpoint. It is important to note that in this methodology problems again arise when we try to treat classically phenomena that are essentially quantum mechanical in nature.

Table 1
Comparison of solution dipole moments calculated with classical [a] and hybrid quantum-mechanical [b] methods (D)

Solute	Vacuum μ	Classical μ		Quantum hybrid μ		Difference
		induced	total solution	induced	total solution	
water	1.857	0.827	2.685	0.605	2.492	0.193
methanol	1.626	0.617	2.237	0.462	2.088	0.149
methylamine	1.397	1.085	2.484	0.523	1.920	0.564
ammonia	1.467 [c]	1.383	2.851	0.747	2.334	0.517
ammonia	1.467 [d]	1.099	2.567	0.747	2.334	0.233

[a] BEM based program HydrEnII with additive polarizabilities on atoms, see ref. [42].

[b] The hybrid method incorporating classical reaction field of the solvent into quantum mechanical DFT calculations [36]. Vacuum dipoles are taken from ref. [36]. Point charges in classical calculations are taken from ref. [32] and linearly scaled to reproduce vacuum dipoles calculated with DFT in ref. [36].

[c] Polarizability on nitrogen $\alpha = 1.094$ Å^3 [42].

[d] Polarizability on nitrogen $\alpha = 0.852$ Å^3 [42].

3. Applications and results

3.1. Compensation between hydration and Coulomb interactions

Such a compensation is a recurrent result of continuum approaches, and we discuss it here and in the following section. If two solutes are brought from infinite separation in water to some separation $\boldsymbol{R}$ in a complex, then the energy of the complex stabilization in solution, $\Delta G^{\mathrm{s}}_{12}(\boldsymbol{R})$, can be expressed as

$$\Delta G^{\mathrm{s}}_{12}(\boldsymbol{R}) = \Delta G^{v}_{12}(\boldsymbol{R}) + \Delta G^{\mathrm{h}}_{12}(\boldsymbol{R}) - \left(\Delta G^{\mathrm{h}}_{1} + \Delta G^{\mathrm{h}}_{2}\right) \tag{14}$$

where the first term on the right-hand side (rhs) corresponds to the energy of the complex stabilization in vacuo, the next term stands for the energy of hydration of the complex, and the sum in the parentheses is the sum of hydration energies of individual solutes. All terms can be calculated either only with a classical continuum theory (including some Lennard-Jones terms at short separations) or with any of its combinations with quantum mechanical calculations.

The first example concerns formation of some of 28 possible nucleic acid base pairs in water [43, and unpublished results]. The old textbooks usually stated that the genetic code is determined by the formation of 'correct' sets of hydrogen bonds in complementary A–T and G–C Watson–Crick base-pairs. In fact, there are 28 hydrogen bonded base-pairs that are structurally different [44, and references therein]. This leads to the question whether the genetic code is determined by a significantly strong stabilization of the Watson–Crick relative to other base pairs. This has been checked for all 28 pairs using Eq. (14) [43, and unpublished results]. The vacuum interaction energy in Eq. (14) has been computed quantum-mechanically with some classical corrections (see legend to Table 2), and hydration energies were computed using our continuum method [9] (solute polarization has not been included, and hydration entropy was not accounted for). The results of calculations for some base pairs hardly suggest any simplistic explanation of the origin of the genetic code. There are seven base pairs within 2 kcal/mol spread of stabilities and about twenty are within 4 kcal/mol. The accuracy of

Table 2
Calculated stabilities of some nucleic acid base-pairs

Base pair [a]	Ranking [b]		Contributions to the free energy of the pair [c]			
	$\Delta E_{12}^{\mathrm{quant}}$	solution	$\Delta E_{12}^{\mathrm{quant}}$	$\Delta H_{\mathrm{el}}^{\mathrm{hydr}}$	$\Delta H_{\mathrm{np}}^{\mathrm{hydr}}$	$\Delta G^{\mathrm{s}}_{12}$
GG(IV)	8	1	−14.70	5.17	2.65	1.12
AC(I)	6	2	−15.80	6.52	2.59	1.31
CC	3	3	−17.91	8.82	2.63	1.54
GC(WC)	1	4	−21.92	11.54	3.13	1.55
GC(II)	5	5	−15.97	7.59	2.67	2.29
AA(II)	16	6	−12.96	4.82	2.60	2.46
AT(WC)	14	7	−13.13	5.37	2.85	2.59
GG(I)	2	10	−21.27	14.06	2.84	3.63
TC(I)	18	11	−12.12	4.65	3.12	3.65
TT(III)	24	15	−10.24	3.77	2.72	4.26

[a] For the nomenclature of the base-pairs see ref. [44]; WC stands for Watson–Crick pairs.

[b] The ranking is from the lowest energy towards the highest one; the first ranking is according to the vacuum interaction energy; the second ranking is according to the base pair stability in water.

[c] The vacuum interaction energies were calculated with SCF MINI-1 basis set corrected for BCCE, dispersion energy, correlation change in the electrostatic energy (see refs. [44–45] and references therein), and zero point energy [46]. Changes in the hydration energy were calculated with method described in ref. [9], with partial charges on the nuclei obtained from fitting to the electrostatic potentials [47a]. The stabilities of pairs in the last column contain the loss of the rotational, translational and vibrational entropies; for the Watson–Crick pairs their values (8.8 kcal/mol for GC and 7.5 kcal/mol for AT) were taken from ref. [47b], and for all other pairs were estimated to be 8 kcal/mol.

the calculations is hardly better than ≈ 2 kcal/mol. However, the spread of stabilities is so narrow that it cannot support an expectation that the genetic code may be determined by a specificity at the base pair level.

Regardless of their particular focus, the calculations contain the result of a general importance: even if the spread of stabilities of hydrogen bonded complexes is large in vacuum, it is significantly smaller in solution. For the data of Table 2 this spread narrows from 11 to 3 kcal/mol. As a rule the better two bases interact with each other the better they interact also with water when separated. Thus, a better electronic complementarity is usually compensated by a larger loss of hydration. The typical examples are two GC and two GG base pairs in Table 2. GC(WC) is 5–6 kcal/mol more stable in vacuum than GC(II), but this is compensated by about 4 kcal/mol difference in hydration enthalpy in the opposite direction. The change is even more dramatic for GG pairs. In vacuum GG(I) is 6.5 kcal/mol more stable that GG(IV), but it is destabilized relative to GG(IV) by 9 kcal/mol larger loss in hydration enthalpy. This reverses the stability ranking of these base pairs in solution relative to that in vacuum. Thus, ranking of complexes in solution cannot be done on the basis of even the best calculations (as well as experiments) in vacuum.

Other examples concern with attempts to evaluate the energetics of the hydrogen bond formation in short protein fragments. Fig. 1 depicts two three residue fragments of RNase A that form two interfragment hydrogen bonds in the crystallographic structure of the protein. We were interested in an estimate of the energy of formation of the hydrogen bond between CO group of residue Thr3 and NH group of residue Lys7. N7–O3

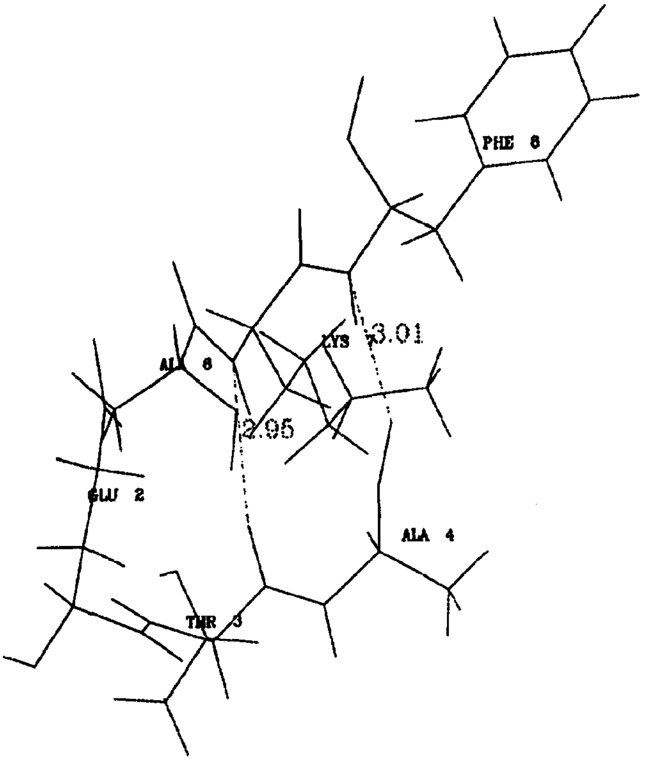

Fig. 1. Electrostatics of the formation of main-chain hydrogen bond CO3-NH7 in RNase A. Fragments 2–4 and 6–8 are depicted in their crystallographic conformation in RNase A [48]. In the calculations partial charges [49] are on atoms C_α, C, O, H_α of Thr3 and N, H of Ala4; on C, O of Ala6 and on N, H, C_α, H_α of Lys7. Calculated hydration energies are: fragment 2–4: −5.37 kcal/mol; fragment 6–8: −4.85 kcal/mol; complex: −6.67 kcal/mol; Coulomb interaction between two fragments: −4.20 kcal/mol.

distance in the crystallographic structure is 2.95 Å, which is close to the ideal length of the hydrogen bond. To avoid end effects partial charges from Amber [48] were placed only on peptide units containing hydrogen bonding groups and on adjacent Cα atom to keep each fragment electrically neutral. Electrostatic part of the enthalpy of hydration has been calculated for the isolated fragments and for the complex. The interfragment vacuum binding energy included only the coulomb interactions between the charged atoms and equaled −4.2 kcal/mol. However, 3.55 kcal/mol of hydration enthalpy is lost upon the complex formation. Thus, the electrostatic contribution to the enthalpy of the hydrogen bond formation is only −0.64 kcal/mol.

Fig. 2 depicts two five residue fragments forming four hydrogen bonds in the β-sheet of BPTI. The fragments were kept electrically neutral with Amber partial charges put on the backbone atoms of residues 20–22 and 31–33. The total Coulomb interaction energy between the two fragments is −17.65 kcal/mol. However, 12.74 kcal/mol of hydration enthalpy is lost upon the complex formation, and thus the total electrostatic stabilization by four hydrogen bonds is only −4.91 kcal/mol (see the legend to Fig. 2 for details). This leads to an estimate of −1.23 kcal/mol stabilization of the complex per hydrogen bond. One may attempt to extrapolate these estimates to cases when hydrogen bonds are buried deeper inside proteins than in Figs. 1 and 2. Such an extrapolation leads to expectations that buried hydrogen bonds contribute very little of electrostatic stabilization to proteins (e.g., see ref. [50]). Such suggestions may well be correct at least in some cases, but should be taken with caution as indicated in the next paragraph.

Another estimate of the electrostatic stabilization per hydrogen bond has been done in the study of electrostatic effects in the folding of the C-peptide of RNase A [51]. In contrast to the previous examples where fragments did not change their conformation upon the hydrogen bond formation, the C-peptide was studied in the extended conformation (a model for the unfolded

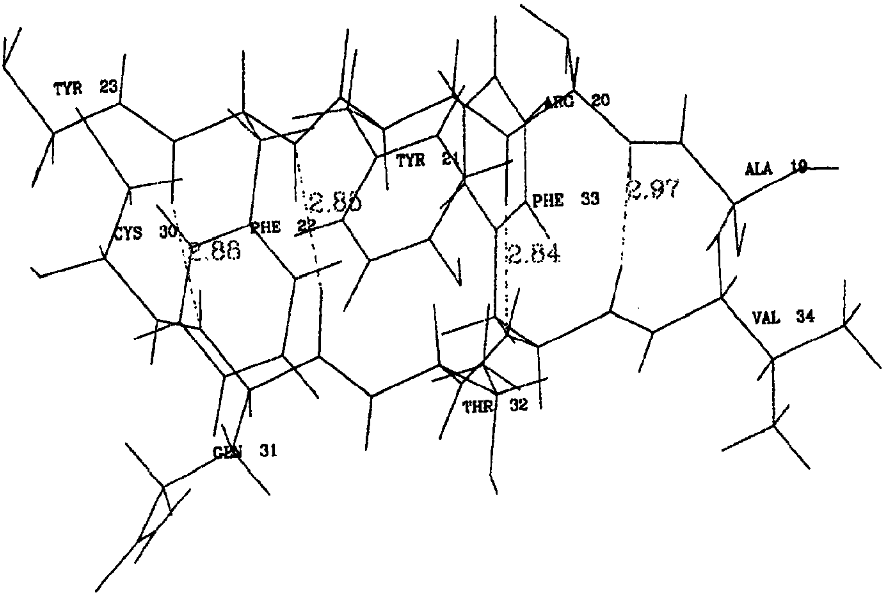

Fig. 2. Electrostatics of the formation of four main-chain hydrogen bonds between fragments 19–23 and 30–34 of BPTI. The fragments are depicted in their crystallographic conformation in BPTI [48]. In the calculations partial charges [49] are on main chain atoms of res. 20–22 and 31–33. Calculated hydration energies are: fragment 19–23: −11.80 kcal/mol; fragment 30–34: −10.58 kcal/mol; complex: −9.64 kcal/mol; Coulomb interaction between two fragments forming four hydrogen bonds: −17.65 kcal/mol.

state) and in the α-helical one [51]. In a subset of calculations partial charges were placed only on the main chain and it was kept electrically neutral. In the calculations utilizing the same AMBER charges and the same $D_{\mathrm{in}} = 1$ as the previous examples, the electrostatic α-helix stabilization per hydrogen bond is ≈ 2.3 kcal/mol. This is 2–3 times larger than in the previous examples. The gain in coulomb energy upon the helix folding is 20 kcal/mol and the loss in hydration energy is only 4 kcal/mol. It is interesting to note that two fragments in Fig. 1 are parts of the same α-helical C-peptide. This seems to stress that the degree of Coulomb-hydration compensation may strongly depend on the reference state (helical in Fig. 1 and extended in ref. [51]). The effect may as well disappear as demonstrated by the calculations for the helix–coil transition of the C-peptide with partial charges on the main chain from ref. [52]. In these calculations hydration energies of the extended and folded α-helical C-peptide are practically identical: −29.0 and −29.4 kcal/mol respectively. Thus, one should be careful with generalizations as the effects may depend on the processes studied and parameters (i.e. partial charges) employed. The picture may change further when more reliable charge distributions and polarizabilities will be used in the calculations.

3.2. Mean potentials and probability distributions

The compensation between Coulomb and hydration energies as a function of separation between polar groups can be manifested in specific shapes of mean interaction potentials between such groups in solution (e.g. see ref. [10]). Here we show that mean interaction potentials (i.e. potentials averaged over configurations of the solvent) between polar groups in solution often have both the contact and the water separated minima. This, however is not necessary the case, and such potentials can be completely repulsive despite strong electrostatic attraction in vacuum.

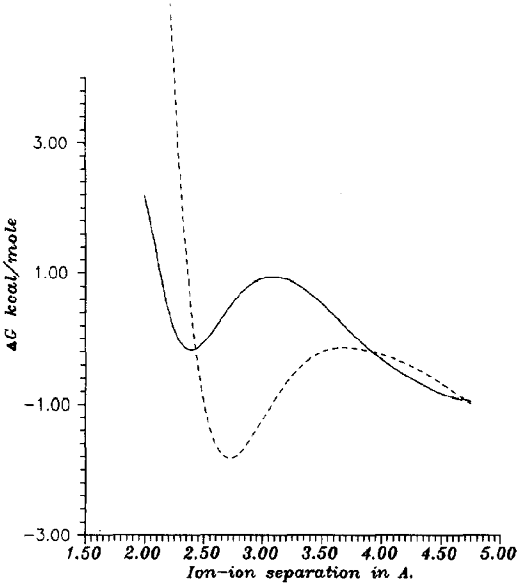

Fig. 3. Mean potentials (or 'potential of mean force') between the ions in pairs Li^+Cl^- (solid line) and Na^+Cl^- (dashed line). Parameters used in the computations are the same as in ref. [10], but calculations have been performed with HydrEnII program.

Mean potentials between Li^+ and Cl^-, and between Na^+ and Cl^- are shown in Fig. 3. The calculations were performed as described in ref. [10] with the dielectric boundary represented (as in all our applications of the continuum electrostatics) by the 'molecular' surface [53–55]. Both curves in Fig. 3 exhibit one minimum at approximately ion–ion equilibrium separation, and another minimum at approximately the distance where one water molecule fits between the ions (water separated minimum). Individual contributions (the hydration and Coulomb energies relative to infinite separation between the ions, and repulsion [56]) are shown in Fig. 4 for Na^+Cl^- pair. It is clear from curves for individual contributions that all of them are monotonic. The two minima and a maximum between them result from differences in rates of change in these contributions as a function of ion–ion separation. The barrier between the two minima appears in the sum of the Coulomb and hydration contributions. The repulsion contribution modulates the curve and does not allow the Coulombic attraction to diverge at short separations (in fact a sum of the Coulomb and repulsion contributions can produce the double minimum profile if properly shifted relative to each other). It is interesting to note that the contact minimum is deeper for

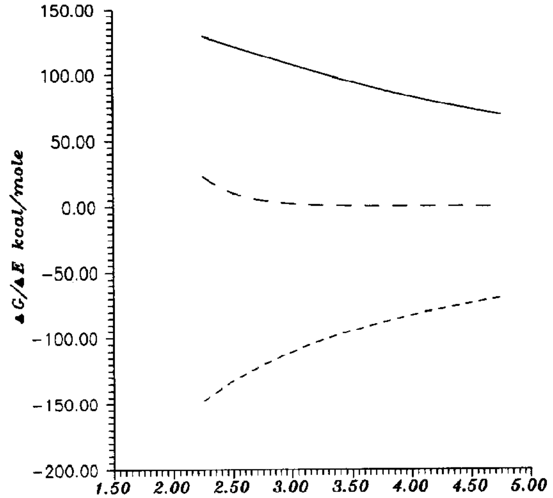

Fig. 4. Different contributions to the mean potential between Na^+ and Cl^-: electrostatic hydration free energy (solid line), Coulomb energy (short dashes), repulsion energy (long dashes with stars).

Na^+Cl^- than for Li^+Cl^- [10]. This trend of increasing depth of the contact minimum with increasing size of the cation is preserved for larger ions (K, Cs) [10]. NMR measurements show a decrease in the probability of finding two ions in proximity of each other along the same series [M. Holz, personal communication].

It is of interest to find out whether this phenomenon is exhibited for all pairs of positively and negatively charged particles. Calculations for $Cu^{2+}Cl^-$ pair [10] also exhibited two minima, but the contact minimum was a few kcal/mol above zero. Here we tried to compute mean potentials in solution for LiCl and NaCl pairs with the same parameters as for ion pairs [10] but reducing the charge twofold on one of the particles. To our surprise a contact minimum did not appear. The total mean potential for $Na^+Cl^{0.5-}$ and its decomposition into different contributions are shown in Fig. 5. It is possible to see that a contact minimum appears for the sum of the hydration and Coulomb contributions, but it is wiped out by the repulsion contribution.

An attempt to substitute $Cl^{-0.5}$ by a dipole of $\pm 0.5e$ placed in the centers of two Cl-sized spheres shifted by 1 Å relative to each other also did not produce any contact minimum. Again the sum of the Coulombic and hydration terms produces a shallow minimum but it is wiped out by the repulsive contribution.

In our calculations of interactions between a water molecule and various cations we found that the depth of the contact minimum increases with decreasing size of the cation [14] (see Fig. 6). This trend is in the opposite direction to that observed for Cl^- alkali-metal pairs (the depth of the contact minimum decreased for smaller cations). To elucidate reasons for this reversal we calculated mean potentials between a cation (Li^+ or Na^+) and a hypothetical small anion of the size of water oxygen. The Lennard-Jones potential was constructed as in ref. [14]. The depth of the minimum of this potential was (as in ref. [14]) chosen to be $\varepsilon = 0.1$ kcal/mol. Parameter σ was chosen so that the sum of the Coulomb, hydration and Lennard-Jones contributions have a minimum at a preset separation (2.03 for Li^+O^- and 2.37 for Na^+O^- pairs [14]). Computations lead to curves for mean potentials with both the contact and the water separated minimum (Fig. 7). The contact minimum for Li^+O^- is ≈ 1.5 kcal/mol deeper than the contact minimum for Na^+O^- potential. This provides a sought answer to the

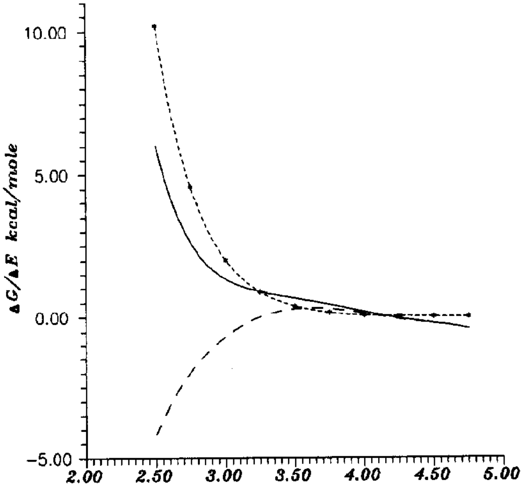

Fig. 5. Mean potential between Na^+ and $Cl^{-0.5}$ (solid line), the sum of hydration and Coulomb contributions (long dashes), the repulsion energy (short dashes).

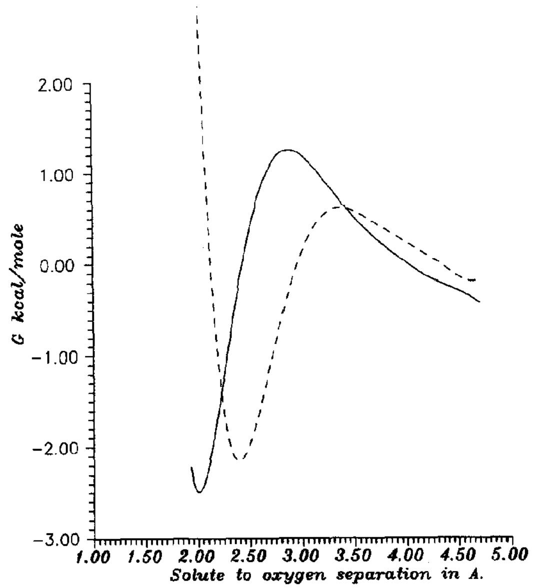

Fig. 6. Mean potentials between a water molecule and Li^+ (solid line) and Na^+ (dashed line). The water molecule is in the optimal orientation for the water–ion interactions.

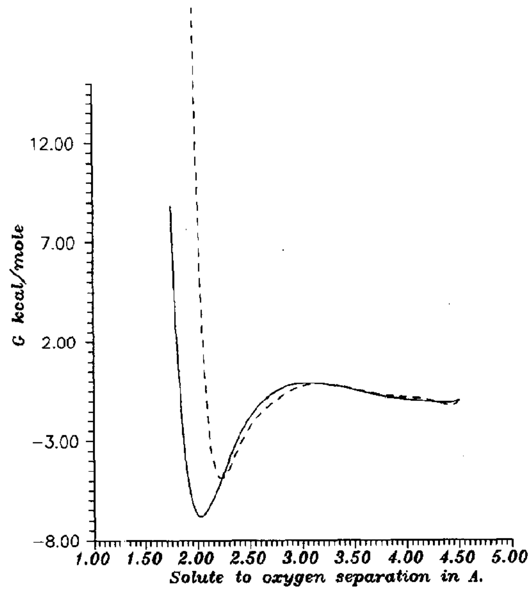

Fig. 7. Mean potentials between the ions in pairs Li^+O^- (solid line) and Na^+O^- (dashed line).

reversal of trend in depths of contact minima. When cations pair with a larger anion the contact minimum becomes deeper for larger cation; when they pair with a smaller anion the trend reverses itself and the contact minimum becomes deeper for a smaller cation. There may be other mechanisms that would be interesting to investigate, but this is one of them. Mean potentials for cation-water pairs follow the same trends as cation–O^- pairs, but cation–water contact minima are shallower.

Is this double-well character of mean potentials characteristic only for simple model systems

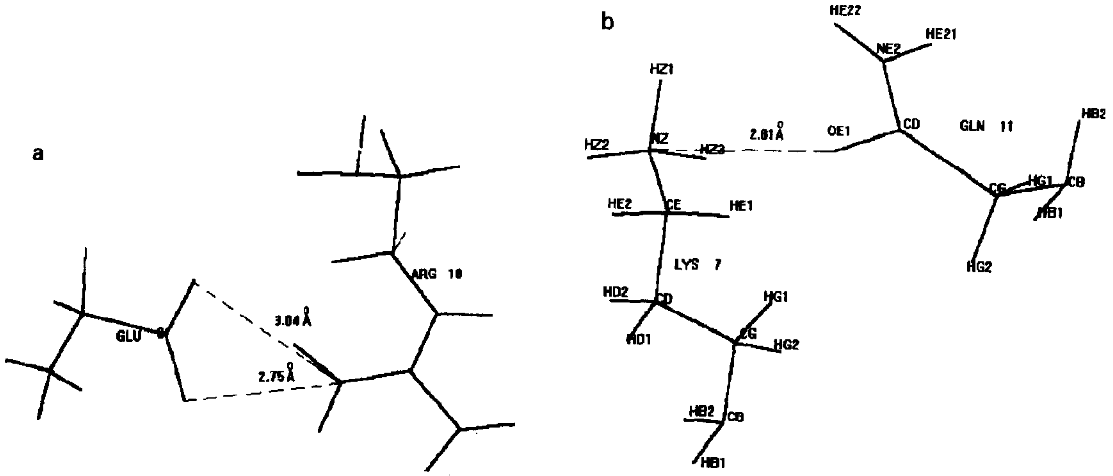

Fig. 8. (a) Side chains of $Glu2^-$ and $Arg10^+$ from RNase A. One of NH2 groups of Arg interacts with both oxygens of Glu; (b) side chains of Lys7 + and Gln11 from RNase A. The amino-group of Lys interacts with one of polar groups of Gln.

or also for interactions between, say, protein side chains? Two pairs of polar protein side chains are shown in Figs. 8a and 8b. Both pairs are taken from the C-peptide of RNase A and relative positions of their polar atoms are subjected to short energy optimization with Amber parameters. Mean potential between Glu2 and Arg10 is shown in Fig. 9, and that between Lys7 and Gln11 is shown in Fig. 10. Both figures show deep contact minima with the water separated minimum more pronounced for the ion-pair. The barriers between the minima are quite low (0.5–0.75 kcal/mol) as approached from an infinite separation. These potential curves are obtained by relative translation of the groups along selected directions (see legends to Figs. 9 and 10). Not all translational directions produce minima with barriers between them, and some of them can be employed in actual conformational changes in proteins.

The results reported in this chapter still leave us with a question whether they correspond to reality closely enough. The experimental data mentioned above is scarce, and the only alternative is to compare our results to those from other theories, e.g., molecular theories. A problem with this way of verification is that molecular theories often disagree with each other [30]. A high similarity of our mean potentials for alkali–chloride ion pairs with RISM results [56] has been demonstrated [10]. On the other hand for mean potentials between like-charged ions our computations did not predict near-contact minima in contrast to RISM [56] and molecular simulations [57]. It has been suggested [58] that for a like-charged ion pair the quadratic dependence of the solvation thermodynamics on the solute charge (becoming $\approx (2q)^2$ for a like-charged pair) more than compensates for the Coulombic repulsion [58]. We do not find this suggestion to be correct in calculations for hard core ions for which equilibrium ion–water distance does not depend on the pair's charge. The Coulombic repulsion happily dominates the potential. For soft core ions the situation may dramatically change [10], and a 1–2% contraction of the ionic cavity (equilibrium ion–water separation) in the doubly charged pair relative to that of a monomer can easily lead to a minimum at near contact separations [10]. More recent molecular studies show that pair potentials of mean force are rather model dependent, which to a significant extent disqualifies them as a standard for comparisons. Thus, the maximum we can state now is that mean potentials for oppositely charged ion-pairs and for ion–water pairs in solution obtained with the continuum approach are at

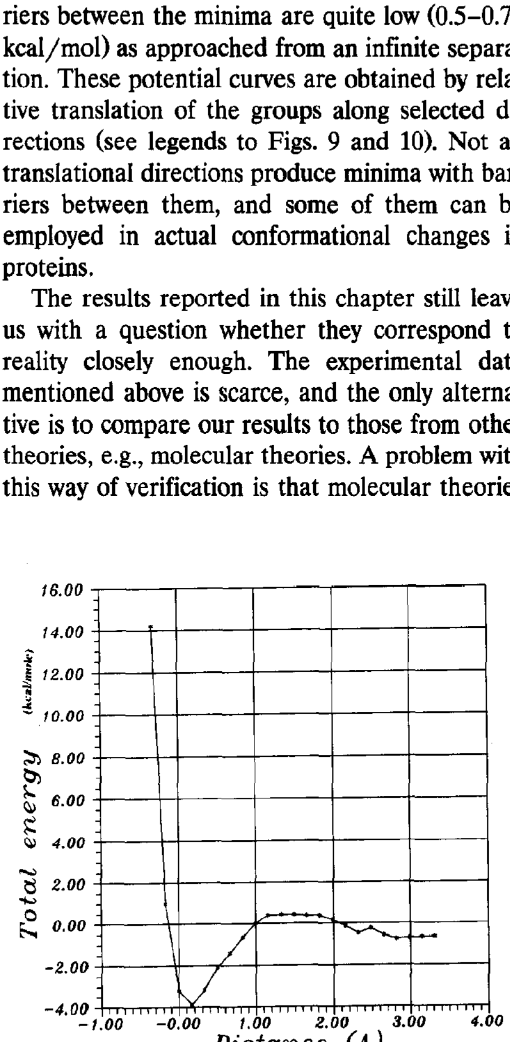

Fig. 9. Mean potential between Glu2 and Arg10 when they are shifted from their position in Fig. 8a along the line from CB2 to CZ10 atoms.

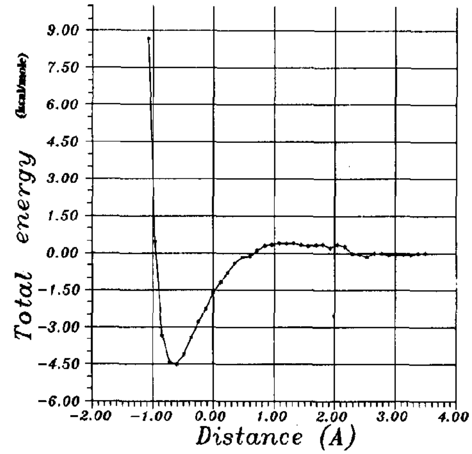

Fig. 10. Mean potential between Lys7 and Gln11 when they are shifted from their position in Fig. 8b along the line from NZ7 to CD11 atoms.

least qualitatively similar to those from molecular theories.

Another example of similarity between results of the continuum approach and those of molecular simulations has been found for relative probabilities of orientations of a water molecule near a molecule of an inert gas (Fig. 11) [13]. But again the degree of agreement is very high with some molecular studies and only qualitative with the results of the others [13].

There is one important case where the mean potential from the continuum method makes a clear physical sense but is not similar to the corresponding potential from molecular studies. This is the mean potential between a water molecule and a non-polar sphere in water (Fig. 12). The main feature of these potentials is that they have positive value when the water molecule is closer to the non-polar spherical particle. Then the potential decreases and reaches its asymptotic value at about the distance between the water and the non-polar sphere when another water can pass between them. The degree of the initial repulsion depends on the orientation of the water relative to the nonpolar sphere. The physical meaning of these potentials is very clear: a water molecule does not like to be near a non-polar particle. The reason for this 'dislike' is a loss of a part of hydration by the water molecule, the part provided in the bulk water by water molecules now displaced by the nonpolar solute. The shape of the mean potential that is observed in our studies closely correspond to liquid density profiles near a wall known as 'wetting by gas' [59]. Mean potentials from molecular simulations have a negative minimum around the contact separation between the water and the solute which then becomes slightly repulsive and then oscillates around zero. This molecular profile is to a significant extent reflecting just the packing of water molecules around the solute which is not described in the continuum model. Nevertheless, the difference between the continuum and molecular result is rather drastic in this case.

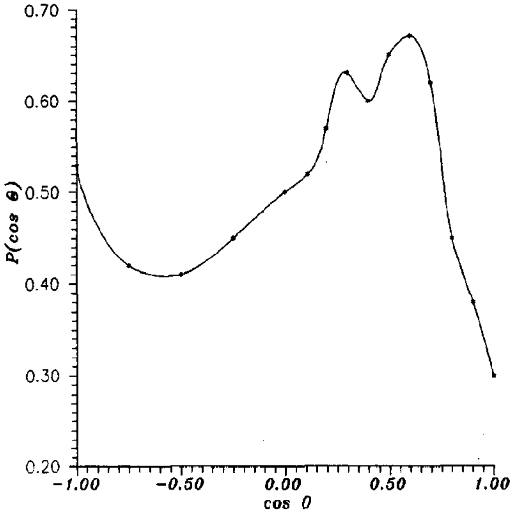

Fig. 11. Relative probabilities of different orientations of water molecule near Ne [13]. Θ is the Ne–O–H angle.

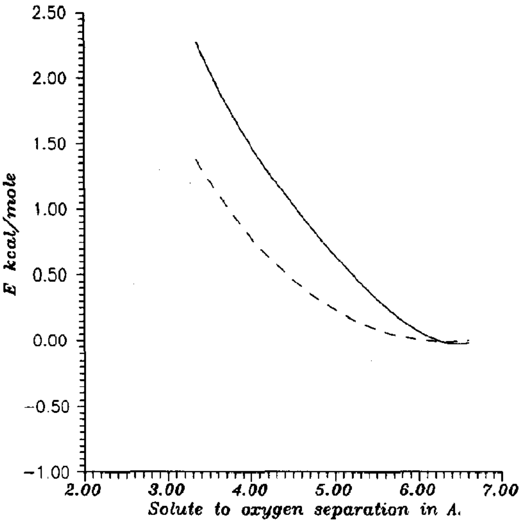

Fig. 12. Mean potentials between a water molecule and a non-polar sphere in water for two different orientations of the water molecule.

3.3. Entropies of hydration

As mentioned in the section on the choice of observables, rather than to calculate the free energy of hydration directly we chose to compute it as a sum of the enthalpic and entropic terms. This allows to clarify some of the specific features of the hydration thermodynamics as shown below.

We concentrate on the configurational contribution to the entropy, assuming that the momentum part is not relevant to the thermodynamics of the solute transfer between different phases [60]. Because in the classical statistical mechanics the configurational entropy is defined only up to an additive constant [61], we calculate the entropy of hydration of a spherical particle as a difference between the entropies of two model configurational probability distributions. These model probability distributions represent the water with an added spherical solute ('main' model) and pure water ('reference' model), correspondingly [14]. The entropy in each of these models is [15]:

$$S = -k\int_V \rho(\boldsymbol{r}) \ln[\rho(\boldsymbol{r})]\ \mathrm{d}V, \tag{15}$$

where $\boldsymbol{r}$ is a point in the configurational space, $\mathrm{d}V$ is its differential element, and $\rho(\boldsymbol{r})$ is the probability density of a configuration $\boldsymbol{r}$

$$\rho(\boldsymbol{r}) = \exp[-E(\boldsymbol{r})/kT]/\Omega, \tag{16}$$

where $E(\boldsymbol{r})$ is the energy of a configuration $\boldsymbol{r}$, and Ω is the configurational integral

$$\Omega = \int_V \exp[-E(\boldsymbol{r})/kT]\ \mathrm{d}V. \tag{17}$$

To greatly simplify the computations of hydration entropies we make two assumptions [13–15]: (a) the total entropy of water in a system is the sum of entropies of individual water molecules; (b) the contributions to $E(\boldsymbol{r})$ of all water molecules in the system other than the selected one can be calculated as solvation energy by using a mean field approximation which represents these water molecules as a continuum dielectric [1,13–15]:

$$\begin{aligned} E_{\text{solvation}}^{\text{water+solute}}(\boldsymbol{r}) &= \tfrac{1}{2}\sum_m q_m^{\text{su}} \sum_j \sigma_j S_j / |\boldsymbol{r}_m - \boldsymbol{r}_j| \\ &\quad + \tfrac{1}{2}\sum_n q_n^{\text{su}} \sum_{m\neq n} \mu_m(\boldsymbol{r}_m - \boldsymbol{r}_n) \\ &\quad / |\boldsymbol{r}_m - \boldsymbol{r}_n|^3, \end{aligned} \tag{18}$$

where su stands for the entire system of a spherical solute and one water molecule; to preserve the spherical symmetry of the system induced dipoles, μ, are only on the atoms of the water molecule and in the second term on RHS of Eq. (18) they interact only with partial charges, q_n^{su}, on the spherical solute. Eq. (18) differs from Eq. (5) only by this second term on its RHS.

In the *main* model the position of the solute particle is fixed. One water molecule is picked up, allowed to run over the space occupied by the system, and allowed to have all orientations. Each such position of the water molecule corresponds to a configuration in our model space.

A total energy value, $E_{\text{main}}(\boldsymbol{r})$, ascribed to each configuration is the sum of energies of interaction between all parts of the system under the study [14]

$$\begin{aligned} E_{\text{main}}(\boldsymbol{r}) &= E_{\text{solvation}}^{\text{water+solute}}(\boldsymbol{r}) + E_{\text{Coulomb}}^{\text{water-solute}}(\boldsymbol{r}) \\ &\quad + E_{\text{Lennard-Jones}}^{\text{water-solute}}(\boldsymbol{r}), \end{aligned} \tag{19}$$

where the first term on the RHS is the energy of interaction of the molecular subsystem of a solute and one water molecule with the continuum dielectric representing the rest of water in the system, and the energy of interactions of the partial charges of the solute with the dipoles induced on the water molecule by the solute and by all other water molecules represented as a continuum; the second and the third terms on the RHS of Eq. (19) are energies of the Coulomb and Lennard-Jones interactions correspondingly between the water and the solute in the subsystem described in a molecular detail. In calculations of entropy of non polar solutes the last two terms in Eq. (19) are set to zero; in calculations for polar solutes they are evaluated as described in ref. [14].

The *reference* model has the same configurational space as the main model. However, the energies of all configurations are the same, $E_{\text{ref}}(\boldsymbol{r})$. The actual value, of the constant $E_{\text{ref}}(\boldsymbol{r})$ does not influence the value of the entropy, S_{ref} (see Eqs. (15)–(17)). For convenience we define [14]

$$E_{\text{ref}}(\boldsymbol{r}) = E_{\text{solvation}}^{\text{water}}(\boldsymbol{r}) + E_{\text{solvation}}^{\text{solute}}(\boldsymbol{r}), \tag{20}$$

where the first and the second terms on the RHS denote energies of hydration in a continuum solvent [13,14,16] of one water molecule and of a solute molecule respectively. In calculations of entropy of non-polar solutes the last term in Eq. (20) is set to zero.

Table 3
Calculated and experimental hydration entropies for noble gases and alkali and halide ions [a]

Solute	He	Ne	Ar	Kr	Xe	Rn	Li^+	Na^+	K^+	Rb^+	Cs^+	F^-	Cl^-	Br^-	I^-
calculated $T\Delta S$	2.23	2.51	3.46	3.68	4.71	5.40	9.76	9.13	4.37	3.74	3.55	11.3	4.03	3.36	3.23
experiment $T\Delta S$	2.40	3.03	4.39	4.86	5.19	5.44	10.1	7.95	5.30	4.66	4.23	9.82	5.38	4.22	2.58

[a] All values are in kcal/mol and correspond to $T = 298$ K. The calculated values are from refs. [14,15]; the experimental values can be found in refs. [13–15] and in references therein.

The *total hydration entropy* of water in the volume V of configurational space is

$$\Delta S_V = (S_{\text{main}} - S_{\text{ref}})N, \tag{21}$$

where N is the number of water molecules that can simultaneously occupy volume V ($N = V/30$) [13]. The way to make calculations for infinite V is described in ref. [14].

Configurations with sterically overlapping solute and water molecule are included in the calculations [15]. These configurations are treated in two different ways: (1) they are assigned the energy of $E_{\text{ref}}(r)$; (2) they are assigned high positive energy. The first treatment assumes that water molecules that occupy these configurations in the reference model (in the absence of the solute) are transferred somewhere else in the bulk water in the main model. Within our model this treatment closely corresponds to the solute transfer at constant pressure. The second treatment forces water molecules out of the solute excluded area in the main model, and decreases the total volume occupied by water in the main model compared to that in the reference model. Within our model this treatment closely corresponds to the solute transfer at constant volume.

Our definition of hydration entropies in Eqs. (15)–(17) and (21), suggested in ref. [13], is equivalent [15] to Eq. (42) of ref. [62] derived later and using water–solute pair correlation function, $g(r)$, for calculations of hydration entropies of nonpolar solutes,

$$\Delta S = -\frac{k(N-1)}{V\Theta}\int g_{\text{sw}}^{(2)} \ln g_{\text{sw}}^{(2)}\, \mathrm{d}\boldsymbol{r}_1\, \mathrm{d}\omega_1 - \tfrac{1}{2}k, \tag{22}$$

where $V\Theta$ is a normalization constant for the integral over positions, $\boldsymbol{r}$, and orientations, ω. However, physics of the problem in our approach is reflected in $\rho(r)$ calculated with mean-field continuum approach, and in ref. [62] in $g(r)$ obtained with molecular computer simulations.

Both our approach [13,15] and that of ref. [62] lead to good predictions of experimental entropies of hydration of spherical non-polar particles. Our $\rho(r) = g(r)/V\Theta$. For nonpolar solutes $g(r)$ is easily expressible through our mean potentials between a nonpolar sphere and a water molecule. Thus, it appears that both an accurate $g(r)$ from molecular simulations [62] and our mean potential, which is drastically different from the molecular mean potential for the same system (see the previous section), lead to equally accurate predictions of experimental hydration entropies [13–15,62]. It may suggest that there is some systematic correspondence between these two shapes of mean potentials that makes them indistinguishable in expressions for hydration entropies. E.g., many different mean potentials (or probability functions) may give the same resultant hydration entropy. It may be enough to get right only some integral features of such potentials to correctly predict experimental values. There is, however, an element of surprise in this particular equivalence of rather different mean potentials. It may require some further analysis.

3.4. Do hydration entropies depend on the charge of the solute?

This question is of interest not only from a general theoretical point of view but also in a more practical context of computing hydration entropies of molecules with complex distributions of charge. If the dependence on the solute charge is strong and detail-sensitive then practical computations may become complicated and costly.

We already have shown that our computations lead to a good agreements between the calculated and experimental hydration entropies of noble gases [13,15] as well as for alkali and halide ions [14,15]. These results are summarized in Table 3 to give support to our findings for spherical particles that do not have clear experimental analogs. In the following we will not further concentrate on the agreement with experimental data but rather on more general implications of our results. In this subsection we concentrate on the influence of the solute charge on hydration entropies.

The results of our calculations of hydration entropies of spherical solutes with charges $\pm e, \pm \frac{1}{2}e$ and 0.0 e (uncharged) are listed in Table 4 for different radii of the solutes. The most striking feature of these results is that for the van der Waals radius of 2 Å all solutes have similar hydration entropies regardless of their charge. In fact, they all agree within ≈ 1 kcal/mol. The same degree of agreement holds for half charged and non-polar solutes with radii below 2 Å.

The next important feature of the results in Table 4 is that starting with the radius of 2 Å hydration entropies for non-polar and positively charged solutes coincide within 0.5 kcal/mol. Hydration entropies for the negatively charged solutes with radii larger than 2 Å fall below the corresponding values for non-polar and positively charged solutes. This difference in properties of positively and negatively charged solutes comes from different definitions of their cavity radii that follows from our approach [1,8,9]. As mentioned above, cavity radii of anions are similar to their ionic radii (which in their turn are similar to their van der Waals radii) while for cations the cavity radii are similar to their covalent radii [8,9]. The difference arises from the asymmetry of the water molecules comprising the solvent and producing electron density distributions (for simplicity we can call them just 'charge distributions') that are profoundly different around ions of opposite charge [8,9]. This leads to larger cavity radii for cations than for anions with the same ionic (van der Waals) radii. Consequently, water molecules next to such cations lose more of their hydration that next to anions with the same ionic radii. This in turn leads to a larger variation in the magnitudes of probabilities in Eqs. (16) and (17) and thus to larger hydration entropies given by Eq. (21) (note that entropy is the highest for chaotic systems at equilibrium where all probabilities are similar; increase in the variation of probabilities, which can be viewed as an increase of some sort of order, leads to a decrease in the entropy of the 'main' model [13]).

Table 4
Entropies of hydration of spherical particles of different charges and radii [a]

Charge	Solute van der Waals radius in Å, and $-T\Delta S$ of hydration at 298 K				
	1.0 Å	2.0 Å	3.0 Å	4.0 Å	5.0 Å
$0.0e$	1.33	3.72	6.72	10.40	14.82
$+e$	8.71	3.77	6.26	9.87	15.17
$+\frac{1}{2}e$	2.13	3.24	6.27	10.06	15.27
$-e$		3.79	3.80	5.26	
$-\frac{1}{2}e$	1.94	2.52	2.96	5.03	

[a] All entropies of hydration (kcal/mol) were calculated with our method as described above and in refs. [13–15]. To obtain solute–water equilibrium separation one should add the radius of water (1.4 Å) to the listed van der Waals radius of the solute, e is an absolute value of the charge of electron.

We have argued [15] that for some large enough radii any differences between anions, on one side, and cations and non-polar spheres, on the other, must disappear as electrostatic interactions of water molecules with such large particles should become negligible. However, we do not know at what solute radius it actually happens. We have found that if the cavity radius for an anion with 4 Å radius is taken to be the same as for cation or nonpolar solute with the same ionic or van der Waals radius, calculated $T\Delta S$ for such three solutes are indistinguishable from each other. This behaviour is repeated for solutes with negative charges of -0.5 e.

3.5. *Is hydrophobicity determined by hydration entropies?*

Note that except for I^- radii of all ions in Table 3 are smaller than 2 Å. Thus, data in tables 3 and 4 show that for ions with van der Waals radii smaller than 2 Å entropies are more negative than for non-polar or partially charged solutes (see also Fig. 1 of ref. [15]). The data in these tables also show that the transfer of any solute from the gas phase to water leads to a decrease in the entropy of water. For ions with van der Waals radii below 2 Å this decrease in entropy of water is larger in magnitude than for non-polar solutes of the same size. As discussed above, the decrease of entropy of water around a solute with the radius larger than 2 Å is practically identical for non-polar and positively charged ($+e$ or $+\frac{1}{2}e$) solutes of same radii. At some radius larger than 2 Å hydration entropies of negatively charged solutes ($-e$ or $-\frac{1}{2}e$) should become practically indistinguishable from such entropies of other solutes with the same radii. However, for some interval of van der Waals radii above 2 Å the decrease in the entropy of water around negatively charged solutes can be only about a half of that for the non-polar and positively charged solutes of the same size (Table 4).

Thus, the hydration entropy is negative for all solutes, and for solutes with radii larger than 2 Å it is comparable in magnitude for all solutes of the same size. The decrease of entropy of water is even greater around small ions. As large negative hydration entropy is considered to be the cause of the hydrophobic effect [30, and references therein], our results ask for some clarification of the usually accepted distinction between 'hydrophobic' ('disliking to be dissolved in water') and 'hydrophilic' solutes. All solutes are 'hydrophobic' entropically. Thus, 'hydrophilicity' can come only from enthalpic component of the free energy of transfer [15,63] [#4]. This component is well expressed in transfer of polar solutes from non polar (vacuum or non-polar liquid) environment to a polar one (water). The situation becomes less clear in transfer of polar groups from polar water to polar hydrogen bonding environment. In such cases the enthalpy of transfer can become very small as shown above, and the transfer may be driven by negative entropies of hydration as for non-polar solutes. Thus, the free energy of hydrogen bonding in proteins may be-

Table 5

Entropies of hydration per Å² of accessible surface area for spherical particles of different charges and radii (cal/mol Å²) [a]

Charge	Solute van der Waals radius in Å, and $-T\Delta S$ of hydration at 298 K per Å²						
	1.0 Å	1.4 Å	2.0 Å	3.0 Å	4.0 Å	5.0 Å	10 Å
0.0 e [b]	18.4		25.6	27.7	27.7	28.8	30.0
$+e$	120.4		26.0	25.7	26.9	29.5	
$+\frac{1}{2}e$ [c]	29.3		22.3	25.8	27.5	29.7	
$-e$			24.4	15.2	14.4		
$-\frac{1}{2}e$	23.3	18.1	17.3	12.2	13.7		

[a] The data from Table 4 are normalized to the accessible surface area, ASA, of each solute; ASA = $4\pi(R_{\mathrm{vdW}} + 1.4)^2$ [30, and references therein]; additional results for negatively half-charged solute with the van der Waals radius of oxygen (1.4 Å) and for non-polar solute with the Waals radius of 10 Å are added;

[b] For non-polar solutes results obtained with one of the sets of parameters are given; in computations with a different set of parameters results for solutes with 1 and 2 Å radii practically did not change; they increased to 30.0, 30.2, 32.1 and 35.0 cal/mol Å² for non-polar solutes with the radii of 3, 4, 5 and 10 Å respectively; results of still other computations fell between these values and those given in the table; these variations may reflect the accuracy of our method;

[c] In addition calculations have been performed for a solute with parameters of the hydrogen bonding hydrogen (e.g., see ref. [32]) and a small partial charge ($+0.3e$) yielding the hydration entropy of 39 cal/mol Å²; this solute has been thought to model a water molecule, ammonia or a hydroxyl group.

[#4] S. Cabani et al. [63] drew conclusions similar to ours [15] on the basis of their analysis of experimental thermodynamics of transfer within a scheme of additive group contributions. They state (p. 577): "The hydration entropy is always negative and its value is not significantly dependent on the nature of the group. ...In fact, the enthalpy is the most suitable function to distinguish polar from nonpolar groups". We found this statement after our paper [15] based on the continuum theory was in press and we were working on ref. [32]. However, it is rather difficult to understand why apparently nobody paid attention.

come mainly entropy driven [15,64]. These conclusions, of course, can be so far valid only at room temperature for which the calculations were performed in this work. They currently do not address differences in temperature dependencies of the transfer thermodynamics of different solutes [65,66] (see also below).

3.6. Entropies of hydration at constant volume and at constant pressure

The values in Tables 3 and 4 are calculated assuming gas to water transfer at constant pressure. Data from Table 4 are recast in Table 5 in terms of hydration entropies per Å^2 of the accessible surface area, ASA [30, and references therein].

It is easy to see that hydration entropies per unit surface area change only ≈ 20% for non-polar solutes with radii between 2 and 10 Å, and only ≈ 10% between radii of 3 and 10 Å. The variations are similar in magnitude for positively charged solutes and exhibit more complex behavior for negatively charged solutes as described in the previous section. For solutes with radii smaller than 2 Å trends in $T\Delta S/\mathrm{ASA}$ are drastically different for non-polar and polar solutes. For non-polar solutes we see ≈ 40% increase in $T\Delta S/\mathrm{ASA}$ between solute radii of 1 and 2 Å, while for polar solutes we observe a decrease in $T\Delta S/\mathrm{ASA}$ values. Thus, our results show that the interplay between the charge and the size may lead to a rather complex trends observed experimentally [32]: (a) for alkanes (which can be represented by spheres larger than 2 Å) $T\Delta S/\mathrm{ASA}$ is almost constant; (b) its value can be significantly smaller for the carbonyl oxygen (represented here as negatively half-charged solute) than that for alkanes; (c) it may be higher for groups with hydrogen bonding hydrogens than for alkanes (see the legend to Table 5).

We shall now concentrate on the observations above that $T\Delta S/\mathrm{ASA}$ remains fairly constant for nonpolar solutes with radii larger than 2–3 Å. This observation is valid only under conditions of the constant temperature and pressure (NPT ensemble) at which it was computed. Hydration entropies under constant temperature and constant volume conditions can be obtained from those under the constant pressure within the model assumed for our computations. Our model intrinsically possesses gas-like properties [15]. This comes from inclusion of correlations only in the mean field which is effectively felt as an external field by each individual water molecule. In uniformly distributed gas (at constant temperature) the entropy is defined by its volume [61]

$$S_{\mathrm{gas}} = Nk \ln V_{\mathrm{gas}}. \tag{23}$$

We can use Eq. (23) to calculate the entropy change when the gas volume changes from V_1 to V_2, where $V_1 - V_2 = n_0 V_0 \ll V_1 = NV_0$, V_0 is the partial molecular volume of a gas molecule at normal conditions ($V_0 = 30$ Å^3 for water), N is a total number of gas molecules in the system. Then for a single cavity of volume $n_0 V_0$ in the gas

$$\begin{aligned} T\Delta S_{\mathrm{gas}}^{V_1 \to V_2} &= NkT \ln\left(\frac{V_{2,\mathrm{gas}}}{V_{1,gas}}\right) \\ &= NkT \ln\left(\frac{V_0(N-n_0)}{V_0 N}\right) \\ &= NkT \ln\left(1 - \frac{n_0}{N}\right) = -kTn_0 \end{aligned} \tag{24}$$

(Molar values can be readily obtained by considering N_{Avogadro} of systems with one cavity). The cavity volume $n_0 V_0$ in our calculations is defined analogously to the partial molecular volume of the solute in the Kirkwood–Buff theory (e.g., see Eq. (3.147) in ref. [60]). For water it is equal to the volume of a spherical shell between radii corresponding to the minimum water–water separation and the minimum solute–water separation [15] plus the partial molecular volume of water. Our calculations show that within 2% Eq. (24) gives the difference between hydration entropies calculated at constant pressure and at constant volume. This compression term [60] is about 75% of $T\Delta S$ for solutes with radius of 5 Å, shown in Table 4, and it is ≈ 200% for solutes with radius of 10 Å shown in the same table. Thus, the entropy of hydration at constant volume conditions, $T\Delta S_V$, is more negative than the entropy of hydration at constant pressure, $T\Delta S_P$, (which is a usual experimental condition) by the entropy of compression of ideal gas. Recent analysis of experimental data for methane solutions also suggest a difference of ≈ 1.5 kcal/mol between entropies of transfer at constant pressure and at constant volume [58,67]. While for real liquids the compression entropy may behave in a more complex way than for the ideal gas, Eq. (24) leads to the value of ≈ 1.8 kcal/mol for the same transfer if an equilibrium water–methane separation is 3.4 Å. It may suggest that the entropy of compression of ideal gas is a surprisingly good model for the compression entropy of water. Note that the entropy of hydration at constant pressure is, according to our results, nearly proportional to the accessible surface area of the solute (surface term), while the change to the constant volume conditions adds to it the gas compression term which is proportional to the partial molecular volume of the solute (volume term). This volume term becomes larger than the surface term for solutes with radii larger than ≈ 6 Å. It can also be noted that Eq. (24) is closely related to the entropic correction suggested in ref. [68] but has an opposite sign.

3.7. Are there volume terms in the free energy of hydration?

Let us first consider an ideal gas compressed to the volume of a real liquid. To keep N molecules of the ideal gas in the volume NV_0 (see Eq. (24) and notations to it) the external pressure should be $P = NkT/NV_0 = kT/V_0$. If we insert into this compressed ideal gas a solute with partial molecular volume n_0V_0 inaccessible for the centers of the gas–solvent molecules, then under the constant volume and temperature conditions the entropy of the gas–solvent decreases by the compression entropy of kTn_0 (see Eq. (24)). Under the constant pressure and temperature conditions the volume occupied by the ideal gas does not change ($V = NkT/P = \text{const}$) and, thus, its entropy does not change because it depends only on the volume (Eq. (23)). However, the system would have to expand by the volume $\Delta V = n_0V_0$ against the external pressure $P = kT/V_0$ (see above). This requires the expansion work $P\Delta V = kTn_0$. Thus, for the transfer of inpenetrable solute into the solvent of the compressed ideal gas free energy under either the constant volume or the constant pressure will be significant and proportional to the partial molecular volume of the solute.

Now let us consider a model solvent that behaves like the ideal gas except that it is kept together by its own mean field so that the external pressure is only one atmosphere. Such external pressure corresponds to strongly cohesive liquids (e.g., water). This model solvent closely corresponds to our computational model described above. Insertion of the same solute into this model solvent under the constant volume conditions would lead to the same compression entropy of kTn_0 as in the case of the compressed ideal gas.

However, under the constant pressure the expansion work against the external pressure (one atmosphere) is negligible [15,60]. Ben-Naim argues [60] that for real liquids the $P\Delta V$ volume term becomes significant only for macroscopic solutes. Thus, no work proportional to the volume of the solute is done under the constant pressure conditions. Because the free energy of transfer should be the same under both conditions [60], this requires that the internal energy change due to the compression of the solvent in the constant volume transfer should be negative to compensate the negative compression entropy change [15]. Recent simulations studies of the Lennard-Jones liquid [69] indicate that such decrease in the internal energy upon a compression is possible. The minimum of internal energy for particles with the Lennard-Jones diameter σ corresponds to the packing coefficients between 0.8 and 1.0 [69], which are significantly larger than for the tight packing of hard spheres with the same diameter (0.74 [70]). In our calculations and in real cohesive liquids the mean field is perturbed around the solute leading to effects proportional to the surface area of the sphere with the diameter equal to the solute–solvent equilibrium distance. These effects lead to the free energy of transfer that is nearly proportional to the accessible surface of the solute [15] (the surface term).

Our computations and the discussion above suggest that non-cohesive liquids (e.g., compressed ideal gas or hard spheres) and strongly cohesive liquids (e.g., water or a Lennard-Jones liquid with a deep potential energy minimum) should behave a drastically different way upon a transfer of molecular size solutes. While for the non-cohesive solvents the free energy of transfer is dominated by the volume terms, it is dominated by the surface terms for strongly cohesive liquids. The logic of our argument suggests that the size of the solute for which volume terms become significant will increase with increasing strength of the interactions between the solvent molecules. We should note that for real liquids with interactions deviating from the mean field approximation used in our computations the compression entropy may deviate from its ideal gas behavior. However, as discussed above, the ideal gas compression entropy reproduced the corresponding effect upon the transfer of methane to water within 20%. Other facts that seem to be in line with our reasoning will be presented elsewhere.

It was recently suggested on basis of considerations of a thermodynamic cycle including a compressed ideal gas intermediate that the free energy of transfer of molecular solutes (from the gas phase and other solvents) to water contains a large volume term [68]. We would argue that this suggestion is likely to be correct only for weakly interacting liquids and is most likely to be erroneous for such strongly cohesive solvent as water. Of course, there is a possibility that strongly cohesive liquids behave in a way intermediate between the extremes discussed in this section. This should be verified by molecular theories and simulations. However, we believe that we have shown here that a transfer of suggestions based on the ideal gas behavior to real cohesive liquids [68] can be internally inconsistent and unjustified.

3.8. Temperature dependence of hydration entropies

The temperature dependence of the thermodynamic characteristics of hydration can be important in such phenomena as protein denaturation [65,66]. To address this issue we did a few preliminary calculations to determine whether experimentally observed temperature dependence of the entropies of hydration is correctly predicted by our continuum approach. We did these calculations in a very straightforward fashion accounting for changes only in a few physically obvious parameters.

We performed computations of hydration entropies according to the description given above and in refs. [13–15] at room temperature and at 373 K. The calculations at room temperature were performed exactly as described above and in ref. [15]. For high temperature calculations $T = 373$ K was used in Eqs. (16) and (17). Also the solvent dielectric constant, D_{out}, in Eq. (3) was set to experimental value of the dielectric constant of water at 373 K [71]. Data from the same source indicate that the density of water changes only a few percent between 298 and 373 K. Therefore, we did not change the partial molecular volume of water in our calculations. We also neglected the temperature dependence of the cavity radii (see above).

Within this simplified model our calculations showed a 25% decrease in the entropy of hydration of a nonpolar solute at 373 K as compared to 298 K. The experimental change amounts to $\approx$ 75% [71]. While the trend is predicted correctly, the discrepancy may indicate that the continuum model does not contain a sufficient amount of relevant physical information to reproduce the magnitude of the temperature dependence of the thermodynamic characteristics of hydration. That would indicate one of the areas where we cannot expect the continuum approach to work in a semiquantitative fashion. However, we can still hope that we just have not accounted for the temperature dependencies of all parameters used in our continuum approach that would contribute to the temperature dependencies of the thermodynamic characteristics of hydration. While the question remains open, we just would like to mark the area where prospects of the continuum approach do not seem to be clear enough at present.

4. Conclusions

We have reviewed above physical ideas behind continuum models of the thermodynamics of hydration and their consequences that seemed most striking to us. Hopefully, we managed to demonstrate that the continuum approach leads to a view of hydration thermodynamics very rich in detail and interpretive ideas. We also tried to emphasize possible inconsistencies in the methodology that may lead to problems in future applications but may also indicate areas of possible research and improvement. We hope that our exposition would facilitate a constructive unprejudiced attitude to the continuum approach from those who observe its developments from the outside, as well as more careful and informed attitude on the part of its practitioners and developers.

The view of the thermodynamics of hydration emerging from continuum studies is still heavily clouded and inpenetrable at places. But on the other hand it is broad, often very clear, and so far always challenging. We feel thrilled and intrigued, and hope that the readers of this Special Issue would be intrigued and challenged too.

Acknowledgement

We thank M.E. Paulaitis, L.R. Pratt, T. Lazaridis, B. Honig, P.J. Rossky and, especially, B.K. Lee for helpful discussions, and B. Rashin and I. Tsinman for help with computations.

References

[1] A.A. Rashin, J. Phys. Chem. 94 (1990) 1725.

[2] K.A. Sharp and B. Honig, Ann. Rev. Biophys. Biophys. Chem. 19 (1990) 301.

[3] J.A. McCammon and S. Harvey, Dynamics of proteins and nucleic acids (Cambridge Univ. Press, Cambridge, 1987).

[4] M.P. Allen and D.J. Tildesley, Computer simulation of liquids (Clarendon Press, Oxford, 1987).

[5] C.L. Brooks, M. Karplus and B.M. Pettitt, in: Advan. Chem. Phys. Vol. 71. Proteins: a theoretical perspective of dynamics, structure, and thermodynamics (Wiley, New York, 1988).

[6] D.L. Beveridge and F.M. DiCapua, Ann. Rev. Biophys. Biophys. Chem. 18 (1989) 431.

[7] J.-P. Hansen and I.R. McDonald, Theory of simple liquids (Academic Press, New York, 1986).

[8] A.A. Rashin and B. Honig, J. Phys. Chem. 89 (1985) 5588.

[9] A.A. Rashin and K. Namboodiri, J. Phys. Chem. 91 (1987) 6003.

[10] A.A. Rashin, J. Phys. Chem. 93 (1989) 4664.

[11] A.A. Rashin, J.R. Rabinowitz and J.A. Banfelder, J. Am. Chem. Soc. 112 (1990) 4133.

[12] A.A. Rashin, Intern. J. Quantum Chem. Quantum Biol. Symp. 15 (1988) 103.

[13] A.A. Rashin and M.A. Bukatin, J. Phys. Chem. 95 (1991) 2942.

[14] A.A. Rashin and M.A. Bukatin, J. Phys. Chem. 97 (1993) 1974.

[15] A.A. Rashin and M.A. Bukatin, J. Phys. Chem. 98 (1994) 386.

[16] M. Gilson and B. Honig, Proteins 4 (1988) 7.

[17] V. Mohan, M.E. Devis, J.A. McCammon and B.M. Pettitt, J. Phys. Chem. 96 (1992) 6428.

[18] M. Orosco, W.L. Jorgensen and F.J. Luque, J. Comput. Chem. 14 (1993) 1498.

[19] R. Zauhar and D. Morgan, J. Comput. Chem. 11 (1990) 603.

[20] B.J. Yoon and A.M. Lenhoff, J. Comput. Chem. 11 (1990) 1080.

[21] K.A. Sharp, J. Comput. Chem. 12 (1991) 454.

[22] H. Oberoi and N.M. Allewell, Biophys. J. 65 (1993) 48.

[23] T.J. You and S.C. Harvey, J. Comput. Chem. 14 (1993) 484.

[24] J. Tomasi, G. Alagona, R. Bonaccorsi and C. Ghio, in: Modelling of structures and properties of molecules, ed. Z. Maksic (Ellis Horwood, Chichester, 1987) p. 330.

[25] C.J. Cramer and D.G. Truhlar, J. Am. Chem. Soc. 113 (1991) 8305, 8552.

[26] S.C. Harvey, Proteins 5 (1989) 78.

[27] M.E. Davis and J.A. McCammon, Chem. Rev. 90 (1990) 509.

[28] D. Bashford, Curr. Opin. Struct. Biol. 1 (1991) 175.

[29] B. Honig, K. Sharp and A.-S. Yang, J. Phys. Chem. 97 (1993) 1101.

[30] A.A. Rashin, Progr. Biophys. Mol. Biol. 60 (1993) 73.

[31] C.J. Cramer and D.G. Truhlar, Rev. Comput. Chem. 6 (1994), in press.

[32] A.A. Rashin, L. Young and I.A. Topol, Biophys. Chem., this Issue.

[33] C.J.F. Bottcher, Theory of electric polarization (Elsevier, Amsterdam, 1973).

[34] K. Sharp, A. Jean-Charles and B. Honig, J. Phys. Chem. 96 (1992) 3822.

[35] A.A. Rashin and J. Malinsky, J. Comput. Chem. 12 (1991) 981.

[36] A.A. Rashin, M.A. Bukatin, J. Andzelm and A.T. Hagler, Biophys. Chem. 51 (1994) 375.

[37] J. O'M. Bockris and A.K.N. Reddy, Modern electrochemistry, Vol. 1 (Plenum Press, New York, 1977).

[38] J. Applequist, J.R. Carl and K.-K. Fung, J. Am. Chem. Soc. 94 (1972) 2952.

[39] B.H. Thole, Chem. Phys. 59 (1981) 341.

[40] D.N. Bernardo, Y. Ding, K. Krogh-Jespersen and R.M. Levy, J. Phys. Chem. 98 (1994) 4180.
[41] A. Warshel and S.T. Russell, Quart. Rev. Biophys. 17 (1984) 283.
[42] Y.-K. Kang and M.-S. Jhon, Theoret. Chim. Acta 61 (1982) 41.
[43] A.A. Rashin and P. Hobza, Biophys. J. 55 (1989) 420a.
[44] P. Hobza and C. Sandorfy, J. Am. Chem. Soc. 109 (1987) 1302.
[45] M.M. Szczesniak, S. Schreiner and P. Hobza, J. Mol. Struct. 179 (1988) 177.
[46] M.M. Szczesniak and P. Hobza, J. Phys. Chem. 87 (1983) 2608.
[47] (a) U.C. Singh and P.A. Kollman, J. Comput. Chem. 5 (1984) 129;
(b) P. Cieplak, P.A. Kollman, J. Am. Chem. Soc. 110 (1988) 3734.
[48] E.E. Abola, F.C. Bernstein, S.H. Bryant, T.F. Koetzle, J. Weng, ‘Protein Data Bank’, in: Crystallographic Databases – Information Content, Software Systems, Scientific Applications, eds. F.H. Allen, G. Bergerhoff, R. Sievers, Data Commission of the International Union of Crystallography, Bonn/Cambridge (1987).
[49] S.J. Weiner, P.A. Kollman, D.T. Nguyen and D.A. Case, J. Comput. Chem. 7 (1986) 230.
[50] M.K. Gilson and B. Honig, Proc. Natl. Acad. Sci. USA 86 (1989) 1524.
[51] A.A. Rashin, Proteins, 13 (1992) 120.
[52] M.N. Bellido and J.A.C. Rullmann, J. Comput. Chem. 10 (1989) 479.
[53] M.L. Connolly, Science 221 (1983) 709.
[54] M.L. Connolly, J. Appl. Cryst. 16 (1983) 548.
[55] M.L. Connolly, J. Appl. Cryst. 18 (1985) 499.
[56] B.M. Pettitt and P.J. Rossky, J. Chem. Phys. 84 (1986) 5836.
[57] L.X. Dang and B.M. Pettitt, J. Am. Chem. Soc. 109 (1987) 5531.
[58] H.-A. Yu, B. Roux and M. Karplus, J. Chem. Phys. 92 (1989) 5020.
[59] J.P. Hansen and I.R. McDonald, Theory of simple liquids (Academic Press, New York, 1986).
[60] A. Ben-Naim, Solvation thermodynamics (Plenum Press, New York, 1987).
[61] G.H. Wannier, Statistical physics (Dover, NY, 1987).
[62] T. Lazaridis and M.E. Paulaitis, J. Phys. Chem. 96 (1992) 3845.
[63] S. Cabani, P. Gianni, V. Mollica and L. Lepori, J. Sol. Chem. 10 (1981) 563.
[64] A.R. Fersht, TIBS 12 (1987) 301.
[65] G.I. Makhatadze and P.L. Privalov, J. Mol. Biol. 232 (1993) 639.
[66] P.L. Privalov and G.I. Makhatadze, J. Mol. Biol. 232 (1993) 660.
[67] T. Lazaridis and M.E. Paulaitis, J. Phys. Chem. 97 (1993) 5789.
[68] K.A. Sharp, A. Nichols, R. Friedman and B. Honig, Biochemistry 30 (1991) 9686.
[69] J.K. Johnson, J.A. Zollweg and K.E. Gubbins, Mol. Phys. 78 (1993) 591.
[70] B.K. Vainstein, V.M. Fridkin and V.L. Indenbom, Structure of crystals (Nauka, Moscow, 1979).
[71] D.R. Lide, ed., CRC Handbook of Chemistry and Physics, 73rd Ed. (CRC Press, Boca Raton, 1992/1993)

Discussion to the paper by A.A. Rashin and M.A. Bukatin

Comments

By B.M. Pettitt

In general, the implied hierarchy of theory and theoretical progress in the last century on the physical science of solutions found in this paper is disturbing. For one, rather than just by 1985, it seems that by Born’s 1920 paper it was known that the continuum method that bears his name was successful in representing the hydration thermodynamics of ions at some level of accuracy. Admittedly, adding (and judicious choice of) parameters to fit the thermodynamics as have been done recently has improved the fitted representation. A certain amount of phenomenological interpretation of such fitting parameters can, under the best circumstances, be fruitful and informative. This is not, of course, an advance in theory but an advance in phenomenological interpretation in some sense, akin to good engineering.

In a formal sense, the continuum terms in common use are derived from low-order terms in exact expansions. Much work in the last forty years has gone into theories which incorporate higher-order terms including molecular packing effects. The resulting expressions do not often lend themselves as easily to fitting as the analytical or numerical continuum results do. There is often a clear distinction between the model Hamiltonian and the theory (not always true for the continuum cases) and thus not only thermodynamic but structural results from such theories may then be compared with their simulated counterparts. In the case of a continuum method especially where liberties with structural parameters are taken no such test is possible. For the hard sphere case (hard sphere ions in a hard sphere multipolar solvent) effects such as the asymmetry between cations and anions in solution is not reproducible with a continuum method. With soft spheres the arguments are the same but can be clouded by phenomenological reference to the real system, begging the question of agreement. Thus, when the parameters of input are then fixed one may be tempted to equate less than quantitative results for modern theories as meaning that they are not as good as an elaborate continuum model where one is fitting data with a flexible function that contains some correct physics. Such an interpretation or outlook can lead one to add more phenomenological terms to continuum model and abandon attempting to understand the basic causes.

It depends on what you want. If you want a quick guess today about solvation free energies, then I would (and do) use a PB method. If I wanted a method more efficient than simulations from which I also had the chance to derive rules of thumb (asymptotic expansions), then modern theories of the liquid state offer a great deal of hope.

By L.R. Pratt

In discussing ion pair potentials of mean force you note the indication that these properties are sensitive to details of the interaction potentials used in molecular calculations and you suggest that for this reason the ion pair potentials of mean force are less useful as tests for more physical models theories such as dielectric models. Do these sensitivities not indicate a limitation of dielectric models, that they do not utilize many molecular details that molecular calculations would, rather than a limitation of these properties for comparison with approximate theories?

Responses by A. Rashin to Comments

To B.M. Pettitt

One of the purposes of this Special Issue, as I understand it, is to expose divisions of opinions in the field and, when possible, assumptions (and often traditional beliefs) that underlie them. Another purpose is to develop a kind of adequate translation of the 'languages' of different approaches one into another that would allow practitioners of one of the approaches to extract constructive information from results of the other without prejudging them on the grounds of the 'language' they are cast in. Therefore I appreciate your bringing up such differences in opinion (or even scientific philosophy) in an open straightforward way. This makes them amenable to a rational discussion that may aid a more constructive interaction between different approaches.

First I would like to mention that continuum electromagnetic theory developed in the last century by Maxwell and other brilliant scientists is no less fundamental than statistical mechanics developed later by Boltzmann, Gibbs, and other. It may be also worth reminding that last century's continuum scientists tried to denigrate Boltzmann's revolutionary ideas for a quite long time. We may just see a reversal of positions in the current discussion while on much reduced scale in issues and personalities. In saying all this I do not mean to imply that a fundamental theory is necessarily correct outside of the context within which it was originally developed. Neither do I intend to imply that a grandeur of an old giant can always justify faults and mediocrities of its humble descendant, such as the approach that we advocate. Otherwise, we do deal with charge distributions, polarizabilities etc., that are the substance of the electromagnetic theory. Furthermore, the Hellmann–Feynman theorem does tell us that after the electron density distribution is determined the rest is just the classical electromagnetism. I hope that the arguments above may to an extent remove a distinction between the 'theories' and 'good engineering'. I am also unsure that such a distinction is justified: what we do either does or does not help to understand nature. If we can leave all this high philosophy behind, then we are left with a question whether a particular model used and its implementation are physically justified. The question of the agreement with experiment comes next, and I do not think that we differ on that.

It is my impression that a part of your comment stems from your viewing very modelistic concepts of the statistical theory as you practice it as fundamental concepts. I mean spherical solvent molecules with well defined radii, the pairwise additivity, etc. I would maintain that a solvent of hard spheres with point dipoles inside is a useful fiction for your model calculations but that nothing like that exists in reality (see my comments to Pratt's paper in this Issue). In reality any dipolar solvent has molecules with very asymmetric electron density distribution, and this real asymmetry provides well justified reasons for assigning different cavity radii to ions of opposite charge with equal ionic radii, which are just another useful fiction (see my comments to Pratt's paper). Continuum electrostatic theory deals with charge distributions, dielectrics, etc., and it is not obliged to work for such a fiction as a hard sphere with a point dipole inside. It does not mean that such a theory is wrong. It is just not concerned with some artefactual objects. You would prove a fault with the continuum theory that assigns different cavity radii to ions of opposite charge in the solvent of electronically asymmetric molecules if you would observe the charge asymmetry for solvation of ions in solvents of (electronically) spherically symmetric molecules, e.g., liquid argon. However, as follows from the discussion of Pratt's paper in this Issue, such proof is unlikely. As for a parametrization to achieve an agreement with experiment, we try to keep it to a minimum and to verify its meaningfulness with quantum mechanics and any other basic theories we can lay our hands on (see Rashin, Young and Topol in this Issue). I would disagree with your judgment that the current continuum model is elaborate. It uses a small number of justifiable parameters, and we would like to keep it this way to critically evaluate it.

I agree with you that molecular models can provide a wealth of structural data that continuum methods are not equipped to deal with. I also agree that the theory of liquid that you practice is a powerful and useful tool as can be judged by your comment to Ben-Naim's paper in this Issue. Your comment can appear to be decisive for the current polemic on the role of volume terms in hydration, and I do not know another approach that could produce so important results with such an ease. I also agree that molecular models should provide crucial checks for less detailed models such as the continuum ones. However, we should concentrate on physically meaningful issues and not on consequences of particular modelistic assumptions (like hard sphere solvents). I hope that we may understand each other better as a result of this discussion, and I am looking forward to your decomposition of the volume effect demonstrated in your comment to Ben-Naim into entropic and enthalpic contributions.

To L.R. Pratt

Generally I would agree with you, but with some qualifications. A picture provided by molecular theories is richer in detail than that from inherently simpler continuum models. However, as you note yourself in your paper in this Issue, simpler models can be physically more transparent. There can be certain advantage in a simpler model with a limited potential for modifications: you should guess it nearly right from the start. The continuum model as we practice it has rather rigid limits on the variation of parameters controlled by experiment, quantum mechanics etc. (see our papers in this Issue). Also, while I am not sure that your modifications of the continuum are warranted, you found yourself that qualitative results do not depend on them. On the other hand, we see qualitative differences in potentials of mean force from different molecular studies. I would just be happier to stand on a more firm ground.